Structures of Neutral Au_7, Au_{19}, and Au_{20} Clusters in the Gas Phase

Philipp Gruene,[1] David M. Rayner,[2] Britta Redlich,[3] Alexander F. G. van der Meer,[3] Jonathan T. Lyon,[1] Gerard Meijer,[1] André Fielicke[1*]

[1]Fritz-Haber-Institut der Max-Planck-Gesellschaft, 14195 Berlin, Germany
[2]Steacie Institute for Molecular Sciences, Ottawa, Ontario K1A 0R6, Canada
[3]FOM Institute for Plasma Physics Rijnhuizen, 3439 MN Nieuwegein, The Netherlands

[*]To whom correspondence should be addressed; E-mail: fielicke@fhi-berlin.mpg.de

The unique catalytic properties of gold nanoparticles are determined by their electronic and geometric structures. Here the geometries of several small neutral gold clusters in the gas phase are revealed by means of vibrational spectroscopy between 47 and 220 wavenumbers. A two-dimensional structure for neutral Au_7 and a pyramidal structure for neutral Au_{20} can be unambiguously assigned. The lowering of the symmetry when a corner-atom is cut from the tetrahedral Au_{20} cluster is directly reflected in the vibrational spectrum of Au_{19}.

The finding of Haruta et al. that dispersed gold nanoparticles show pronounced catalytic activity towards the oxidation of CO has triggered a true gold rush in cluster chemistry (*1*). Whereas bulk gold is a symbol of chemical inertness (*2*), many following studies have confirmed the size-dependent reactivity of deposited gold clusters (*3–6*). Small particles of gold differ from the bulk as they contain edge atoms that have low coordination (*7*) and can adopt binding geometries which lead to a more reactive electronic structure (*8*). Thus, the secret of the catalytic properties of gold nanoparticles lies at least partly in their geometric structure. Structural information for deposited gold mono- and bi-layers on titania has been obtained by using high resolution electron energy loss spectroscopy on CO adsorbates (*9*). Determining the three-dimensional structure of deposited gold nanoparticles is more challenging, but has been achieved recently for clusters containing around 310 atoms using aberration-corrected scanning transmission electron microscopy (*10*).

The geometry of nanoparticles can also be studied in the gas phase. The advantage of this approach is the exact knowledge of the clusters' size and the absence of any interaction with the surrounding environment. The properties of such well defined species can thus be modeled very precisely with quantum mechanical calculations. Different experimental techniques exist for the study of free clusters. By measuring the mobility of size-selected gold anions and cations in helium, a transition from two-dimensional to three-dimensional structures has been found (*11, 12*). This transition appears at different cluster sizes for cations and anions and is yet to be determined experimentally for neutral species. A combination of photoelectron spectroscopy and quantum mechanical calculations has revealed fascinating structures of anionic gold species, e.g., cages for clusters containing 16 to 18 atoms (*13*), a tetrahedral pyramid for Au_{20}^- (*14*), and a possibly chiral structure for Au_{34}^- (*15*). These structural motifs have been confirmed by measuring the electron diffraction pattern of size-selected trapped anions (*15, 16*). Although ion mobility measurements, photoelectron spectroscopy, and trapped ion electron diffraction have all added significantly to the understanding of the

geometric properties of free nanoparticles, these methods are restricted to the investigation of charged species.

Here we investigate neutral gold clusters in the gas phase by means of vibrational spectroscopy, which is inherently sensitive to structure. In infrared (IR) absorption spectroscopy the number of allowed transitions is restricted by selection rules, and thus directly reflects the symmetry of the particle. Far-infrared multiple photon dissociation (FIR-MPD) spectroscopy is a proven technique for obtaining the vibrational spectra of gas-phase metal clusters and hence, by comparison with calculated spectra, their geometries (*17, 18*). It is the only technique for structure determination of free metal clusters that is not limited to charged species. Here we explore three representative sizes of neutral gold clusters. With Au_7 we investigate the structure in a size region where the anions and cations are known to adopt planar structures and thereby address a controversy in theoretical studies. In Au_{20} we confirm that the neutral cluster retains the symmetrical pyramid geometry established for the anion. For Au_{19} we directly observe the lowering of symmetry as one of the corner atoms is removed from Au_{20}.

Details of the technique of FIR-MPD have been described elsewhere (*17, 19*). Neutral gold clusters are produced by means of laser vaporization from a gold rod in a continuous flow of helium and krypton (1.5 % Kr in He) at 100 K. Under these conditions complexes of the bare metal clusters with one or two krypton ligands are formed. The molecular beam is overlapped with a pulsed FIR beam delivered by the Free Electron Laser for Infrared eXperiments (FELIX) (*20*). The neutral complexes are ionized by an F_2-excimer laser (7.9 eV/photon) and mass analyzed in a time-of-flight mass spectrometer. Resonance of the FIR light with an IR-active vibrational mode of a given neutral cluster may lead to absorption of several photons. The subsequent heating of the complex results in the evaporation of a loosely bound krypton ligand and a depletion of the corresponding mass spectrometric signal. Recording the mass spectrometric signal while scanning the wavelength of FELIX leads to depletion spectra, from which absorption spectra $\sigma(\tilde{\nu})$ are reconstructed (*21*).

Figure 1A shows the vibrational spectrum of neutral Au_7 obtained by FIR-MPD of its complex with one krypton ligand. A number of bands are found in the region between 47 and 220 cm^{-1} usually having a full width at half maximum of less than 4 cm^{-1} (*21*). This is close to the spectral bandwidth of FELIX, which is about 2 to 3 cm^{-1} and nearly constant over the whole tuning range. The number of peaks implies a rather non-symmetric structure for neutral Au_7. The geometry of Au_7 is established by comparing the experimental spectrum to the calculated vibrational spectra for multiple isomers predicted by density functional theory (DFT) calculations within the generalized gradient approximation (*21, 22*). We find a planar edge capped triangle with C_s symmetry (Iso1) to be lowest in energy. This structure has been reported previously as the global minimum (*23*). A hexagonal planar structure (Iso2) (*24*) and a three-dimensional structure (Iso3) (*25*) have been proposed as lowest energy structures as well, but are computed to be higher in energy in the present study.

The experimental vibrational spectrum unambiguously tests the reliability of the theoretical methods. The calculated spectra are distinctive in the range between 150 cm^{-1} and 220 cm^{-1}. The peak positions of Iso1 fit with experimental absorptions at 165 cm^{-1}, 186 cm^{-1}, and 201 cm^{-1}. Only the relative intensities of the bands do not agree completely, with the central band at 186 cm^{-1} being much more pronounced in the experiment. Figure 1B shows the calculated absorption spectrum of the complex Iso1·Kr, where krypton is bound to the energetically most favorable position of the Iso1 cluster with a bond dissociation energy of 0.09 eV. The positions of the resonances are not changed but the relative intensities are significantly impacted. The three bands are now in excellent agreement with experiment, and, furthermore, all absorptions between 50 cm^{-1} and 150 cm^{-1} become more pronounced (*26*). The calculations reveal all of these vibrational modes to be highly delocalized, involving motion of all atoms in the cluster (see normal mode displacement vectors for the three highest energy vibrations of Au_7 (all in-plane) in Fig. S3).

In principle, multiple isomers can be present in the molecular beam. In that case the spectrum would represent a superposition of their individual contributions. Iso2 has one strong absorption at 185 cm^{-1}, and its presence in the molecular beam could also explain the pronounced intensity of the central peak in the experimental spectrum. Ion mobility measurements, however, exclude the presence of major amounts of additional isomers for cationic and anionic Au_7. We note also that for experimental modes that are not present in the calculated spec-

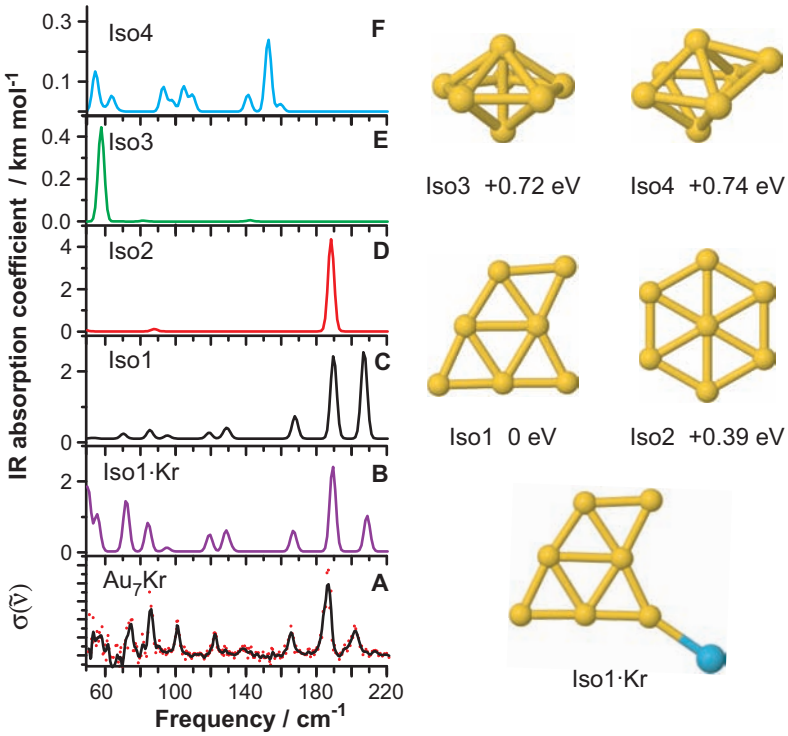

Figure 1: **Vibrational spectra of neutral Au_7.** Panel A shows the FIR-MPD spectrum of Au_7Kr. The red dots represent relative cross sections, $\sigma(\tilde{\nu})$, the average of up to ∼1000 single laser shots at a fixed frequency, while the black line interconnects a binomially weighted 5-point running average, thus accounting for the spectral bandwidth of the IR laser. It is compared to the spectra of four low lying isomers (Iso1–4; panels C-F) obtained by DFT calculations. The peak positions in the experiment are in best agreement with a planar structure of C_s symmetry (Iso1). Considering the krypton ligand in the calculation does not change the structure of the cluster or the positions of the resonances significantly (Iso1·Kr; panel B), but has an effect on the IR intensities which become very similar to those in the experimental spectrum.

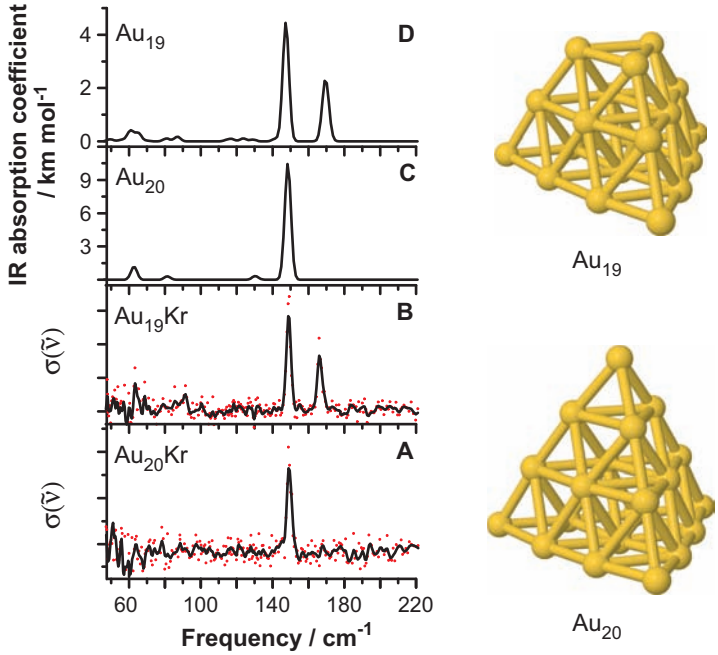

Figure 2: **Vibrational spectra of neutral Au_{19} and Au_{20}.** Panels A and B show the FIR-MPD spectra of $Au_{20}Kr$ and $Au_{19}Kr$, respectively. Calculated spectra for pyramidal geometries Au_{20} and Au_{19} are in excellent agreement with the experiment. The splitting of the degenerate resonance at 148 cm^{-1} for Au_{20} into two peaks at 149 cm^{-1} and 166 cm^{-1} for Au_{19} is due to the lowering of symmetry when going from the tetrahedron to the truncated pyramid.

trum of hexagonal Iso2, e.g., at 165 cm^{-1} and 201 cm^{-1}, the mass spectrometric intensity of Au_7Kr goes down to below 30 % of its original value upon irradiation by FELIX, which sets the upper limit for the abundance of other isomers. Therefore, although a minor contribution of Iso2 cannot be ruled out, the capped triangle can be assigned as the dominant structural isomer of neutral Au_7 present in our experiment.

Upon comparison with the experimentally determined structures of the corresponding ionic species, we find that Au_7 is a cluster size, which changes its geometries for each charge state. Whereas the cation is highly symmetric and corresponds to the D_{6h} structure Iso2 (*12*), the anion forms a threefold edge-caped square (*11*). We find this structure to be a saddle point in our calculations for neutral Au_7 that relaxes into Iso1. The geometrical change as a function of cluster charge corresponds to a lowering of the average coordination as the electron density increases. Whereas the gold atoms in the cation have on average 3.43 nearest neighbors, this value decreases to 3.14 and 2.85 for the neutral and the anion, respectively. The additional electrons obviously favor more open structures.

Having shown that the experimental spectrum, in combination with theory, can be used to identify the geometry of the Au_7 cluster, we moved on to bigger sizes. Photoelectron spectroscopy and quantum mechanical calculations have shown that anionic Au_{20}^- is a pyramid, bearing T_d symmetry (*14*). This structure has also been suggested to be the global minimum for neutral Au_{20} (*14*). The FIR-MPD spectrum we measured of the $Au_{20}Kr$ complexes (figure 2A) is very simple, with a dominant absorption at 148 cm^{-1}, which already points to a highly symmetric structure. The calculated spectrum of tetrahedral Au_{20} is in agreement with the experiment (figure 2C, cf. figure S4 for the IR spectra of less stable isomers). In the FIR-MPD spectrum of $Au_{20}Kr_2$ weaker features occur at low frequencies and are reproduced nicely by theory when including the krypton ligands in the calculations (figure S1). The strong absorption at 148 cm^{-1} corresponds to a triply degenerate t_2 vibration in bare Au_{20} with T_d symmetry.

Theory predicts a truncated trigonal pyramid as the minimum energy structure for neutral Au_{19} (*27*), where the removal of a corner atom of the Au_{20} tetrahedron reduces the symmetry from T_d to C_{3v}. As a direct consequence, the degeneracy of the t_2 vibration of Au_{20} is lifted and this mode splits into a doubly degenerate *e* and an a_1 vibration in Au_{19}. This splitting is observed in the vibrational spectrum of neutral Au_{19} (figure 2). The *e* vibration lies at 149 cm^{-1} and is hardly shifted in comparison to the t_2 mode of Au_{20}. The a_1 vibration is blue shifted by 18 cm^{-1} relative to the t_2 vibration in Au_{20}. The truncated pyramidal structure of Au_{19} can thus be inferred directly from the IR spectrum. We also find the C_{3v} structure of Au_{19} to be a minimum in our calculations and the calculated vibrational spectrum fits the experimental one in terms of peak positions and relative intensities (figure 2D, IR spectra of less stable isomers are shown in figure S5). Again, the modifications in peak intensities induced by the krypton ligands agree well between theory and experiment (figure S2).

We have shown that detailed structural information on small neutral gold nanoparticles can be obtained by means of vibrational spectroscopy. FIR-MPD is the only size selective experimental technique available to date that allows for the structure determination of neutral metal clusters in the gas-phase. It can be used to study the transition of two to three-dimensional structures for neutral gold clusters, as well as to study, for instance, ligand-induced geometrical modifications that are highly relevant in catalysis. With improved sensitivity for heavier masses it will be possible to extend these measurements to larger clusters. Although spectral congestion may prohibit detailed analysis for non-symmetric structures, we can expect symmetric and near-symmetric structures to remain identifiable, as they do for Au_{20} and Au_{19}. For instance it should be possible to answer questions such as is neutral Au_{55} icosahedral or does it have a low-symmetry structure such as has been indicated for the anion (*28*).

References and Notes

1. M. Haruta, N. Yamada, T. Kobayashi, S. Iijima, *J. Catal.* **115**, 301 (1989).
2. B. Hammer, J. K. Nørskov, *Nature* **376**, 238 (1995).
3. M. Valden, X. Lai, D. W. Goodman, *Science* **281**, 1647 (1998).
4. B. Yoon et al., *Science* **307**, 403 (2005).
5. C. T. Campbell, *Science* **306**, 234 (2004).
6. P. P. Edwards, J. M. Thomas, *Angew. Chem. Int. Ed.* **46**, 5480 (2007).

7. C. Lemire, R. Meyer, S. Shaikhutdinov, H.-J. Freund, *Angew. Chem. Int. Ed.* **43**, 118 (2004).
8. G. Mills, M. S. Gordon, H. Metiu, *J. Chem. Phys.* **118**, 4198 (2003).
9. M. S. Chen, D. W. Goodman, *Science* **306**, 252 (2004).
10. Z. Y. Li et al., *Nature* **451**, 46 (2008).
11. F. Furche et al., *J. Chem. Phys.* **117**, 6982 (2002).
12. S. Gilb et al., *J. Chem. Phys.* **116**, 4094 (2002).
13. S. Bulusu, X. Li, L.-S. Wang, X. C. Zeng, *Proc. Natl. Acad. Sci. U. S. A.* **103**, 8326 (2006).
14. J. Li, X. Li, H.-J. Zhai, L.-S. Wang, *Science* **299**, 864 (2003).
15. A. Lechtken et al., *Angew. Chem. Int. Ed.* **46**, 2944 (2007).
16. X. Xing, B. Yoon, U. Landman, J. H. Parks, *Phys. Rev. B* **74**, 165423 (2006).
17. A. Fielicke et al., *Phys. Rev. Lett.* **93**, 023401 (2004).
18. A. Fielicke, C. Ratsch, G. von Helden, G. Meijer, *J. Chem. Phys.* **122**, 091105 (2005).
19. A. Fielicke, G. von Helden, G. Meijer, *Eur. Phys. J. D* **34**, 83 (2005).
20. D. Oepts, A. F. G. van der Meer, P. W. van Amersfoort, *Infrared Phys. Technol.* **36**, 297 (1995).
21. Materials and Methods are detailed in Supporting Online Material available at Science online.
22. R. Ahlrichs, M. Bär, M. Häser, H. Horn, C. Kölmel, *Chem. Phys. Lett.* **162**, 165 (1989); calculated frequencies are uniformly scaled by multiplication with a factor of 1.15.
23. V. Bonačić-Koutecký et al., *J. Chem. Phys.* **117**, 3120 (2002).
24. H. Häkkinen, U. Landman, *Phys. Rev. B* **62**, R2287 (2000).
25. J. Wang, G. Wang, J. Zhao, *Phys. Rev. B* **66**, 035418 (2002).
26. The influence of the rare-gas ligand on the IR absorption intensities is very similar to what has been found in photodissociation studies of cationic gold clusters in the visible region. See: A. N. Gloess, H. Schneider, J. M. Weber, M. M. Kappes, *J. Chem. Phys.* **128**, 114312 (2008).
27. S. Bulusu, X. C. Zeng, *J. Chem. Phys.* **125**, 154303 (2006).
28. W. Huang et al., *ACS Nano* **2**, 897 (2008).
29. The authors acknowledge support from the Cluster of Excellence "Unifying Concepts in Catalysis" coordinated by the Technische Universität Berlin and funded by the Deutsche Forschungsgemeinschaft. This work is supported by the "Stichting voor Fundamenteel Onderzoek der Materie" (FOM) in providing beam time for FELIX. We thank the FELIX staff for their skillful assistance, in particular Jan Pluijgers and René van Buuren as well as Klaus Rademann for providing the cluster source. P. G. thanks the IMPRS: *Complex Surfaces in Material Science* and J. T. L. thanks the Alexander von Humboldt Foundation for funding.

Supporting Online Material
www.sciencemag.org
Materials and Methods
Figs. S1–S5